PERGAMON

International Journal of Solids and Structures 40 (2003) 3603–3619

INTERNATIONAL JOURNAL OF SOLIDS and STRUCTURES

www.elsevier.com/locate/ijsolstr

New planar velocity fields for upper bound limit analysis

A.M. Puzrin [a], M.F. Randolph [b,*]

[a] School of Civil and Environmental Engineering, Georgia Institute of Technology, Atlanta, GA 30332-0355, USA
[b] Centre for Offshore Foundation Systems, The University of Western Australia, Crawley, WA 6009, Australia

Received 7 May 2002; received in revised form 31 January 2003

Abstract

A generalised framework has recently been proposed for derivation of kinematically admissible velocity fields in 3-dimensional upper bound limit analysis in Tresca's material using coordinate transformations. In many cases the approach allows the local dissipation of plastic work to be derived in closed form. The original framework was restricted to orthogonal coordinate systems. However, the present paper extends the approach to allow for variations in plane or radial velocity fields in a direction normal to the field. This important extension allows applications to horizontal loading of circular foundations, or vertical loading of non-circular (e.g. square) foundations.

Keywords: Plasticity theory; Upper bound; Limit analysis; Foundations; Soil

1. Introduction

Upper bound limit analysis has proved a powerful tool in the solution of bearing capacity problems. Historically, most solutions were restricted to 2-dimensional problems, either in plane strain or axial symmetry, although 3-dimensional solutions have also been developed (e.g. Shield and Drucker, 1953; Murff and Hamilton, 1993). In spite of the power of modern finite element software, upper bound solutions still have a role to play, offering a number of advantages in terms of clear physical meaning, simplicity of mathematical calculations, and extension to heterogeneous materials (of particular relevance to geotechnical engineering problems).

Recently, Puzrin and Randolph (2003) have proposed a generalised framework for developing 3-dimensional upper bound solutions for materials satisfying Tresca's failure criterion, ensuring admissibility in respect of zero volumetric strains and adopting local coordinate systems that simplify computation of the maximum principal strain rate. The framework uses orthogonal curvilinear coordinates and allows for derivation of kinematically admissible velocity fields (KAVFs) with new streamline shapes, including derivation of new plane but non-plane-strain fields and new radial but non-axisymmetric fields. However, because of the restriction to orthogonal coordinate systems, derivation of arbitrary 3-dimensional velocity

* Corresponding author. Fax: +61-8-9380-1044.
E-mail address: randolph@civil.uwa.edu.au (M.F. Randolph).

0020-7683/03/$ - see front matter
doi:10.1016/S0020-7683(03)00152-5

fields was not possible. For example, plane fields cannot be derived for footing shapes other than an infinite strip, while radial fields cannot be derived for footing shapes other than circular.

The motivation of this paper is to develop an approach for construction of easily calculable 3-dimensional KAVFs, which would allow greater flexibility in the generation of new upper bound solutions involving, for example, plane velocity fields for a circular footing under horizontal or moment loading, or radial fields for arbitrarily shaped footings. At this stage the analysis will be restricted to the fields with straight or circular streamlines. In spite of this limitation, it is believed that the proposed approach will allow for more accurate approximation of the velocity fields obtained from FE analysis, and hence the development of improved upper bound solutions.

2. General framework for orthogonal fields

The key elements in the framework proposed by Puzrin and Randolph (2003) are summarized briefly below, before extending their work to non-orthogonal systems. The general method for determining an upper bound solution for assemblages of rigid and elastic–perfectly plastic bodies has been presented by Drucker et al. (1951) and Shield and Drucker (1953). For Tresca's yield criterion of constant maximum shearing stress, c_u, the upper bound solution for the surface traction $\mathbf{T} = \{T_x, T_y, T_z\}^{\mathrm{T}}$ is calculated from the following equation:

$$\int_S \mathbf{T}^{\mathrm{T}}\mathbf{v}\,\mathrm{d}S = W(\mathbf{T},\mathbf{v}) = D(\mathbf{v}) = \int_V 2c_u|\dot{\boldsymbol{\varepsilon}}|_{\max}\,\mathrm{d}V + \int_{S_{\mathrm{D}}} c_u|\Delta v|\,\mathrm{d}S \tag{1}$$

where $\mathbf{v} = \{v_x, v_y, v_z\}^{\mathrm{T}}$—the KAVF; $W(\mathbf{T},\mathbf{v})$, the rate of work done by the surface tractions; $D(\mathbf{v})$, the rate of dissipation of work; $|\dot{\boldsymbol{\varepsilon}}|_{\max}$, the absolutely largest principal component of the plastic strain rate; Δv, velocity jump across any discontinuity; S, the surface that bounds the body or the assemblage of the bodies; V, the volume of the assemblage of the bodies; S_{D}, the surface(s) of all discontinuities.

Any variation in the maximum shearing stress, c_u, between the bodies in the assemblage, within the volume of the bodies and along discontinuities must be taken into account in the evaluation of dissipation in Eq. (1). Rigid bodies in the assemblage contribute nothing to the volume integration since the strain rate is zero for a rigid body.

2.1. Orthogonal curvilinear coordinates

Consider Cartesian coordinates (X, Y, Z) and an alternative curvilinear orthogonal coordinate system

$$\begin{cases} x = x(X,Y,Z) \\ y = y(X,Y,Z) \\ z = z(X,Y,Z) \end{cases} \tag{2}$$

defined in such a way that the x-axis (given by intersection between coordinate surfaces y and z) is directed down the streamline of the velocity field. Thus, let the velocity field in coordinate directions x, y and z be defined as $\mathbf{v} = \{u, v, w\}^{\mathrm{T}}$, with:

$$u = u(x,y,z) \quad v = 0 \quad w = 0 \tag{3}$$

For these conditions, the small strain rate tensor in general orthogonal curvilinear coordinates is given by (Boresi and Chong, 2000):

$$\dot{\varepsilon} = \begin{bmatrix} \frac{u_{,x}}{\alpha} & \frac{\alpha}{2\beta}\left(\frac{u}{\alpha}\right)_{,y} & \frac{\alpha}{2\gamma}\left(\frac{u}{\alpha}\right)_{,z} \\ \frac{\alpha}{2\beta}\left(\frac{u}{\alpha}\right)_{,y} & \frac{\beta_{,x}}{\beta}\frac{u}{\alpha} & 0 \\ \frac{\alpha}{2\gamma}\left(\frac{u}{\alpha}\right)_{,z} & 0 & \frac{\gamma_{,x}}{\gamma}\frac{u}{\alpha} \end{bmatrix} \tag{4}$$

where

$$\begin{aligned} \alpha &= \sqrt{(X_{,x})^2 + (Y_{,x})^2 + (Z_{,x})^2} \\ \beta &= \sqrt{(X_{,y})^2 + (Y_{,y})^2 + (Z_{,y})^2} \\ \gamma &= \sqrt{(X_{,z})^2 + (Y_{,z})^2 + (Z_{,z})^2} \end{aligned} \tag{5}$$

and the notation $a_{,b} = \partial a/\partial b$ is adopted.

The incompressibility condition is equivalent to the following differential equation:

$$\frac{u_{,x}}{\alpha} + \frac{\beta_{,x}}{\beta}\frac{u}{\alpha} + \frac{\gamma_{,x}}{\gamma}\frac{u}{\alpha} = 0 \tag{6}$$

which, upon integration, yields the following functional form for the velocity component u:

$$u(x,y,z) = \frac{f(y,z)}{\beta\gamma} \tag{7}$$

where $f(y,z)$ is an arbitrary function of y and z. Thus the incompressibility condition does not place any restrictions on variation of the velocity with the y and z coordinates, but its variation with the x-coordinate depends on the functional form of β and γ.

Application of the above method to a chosen KAVF requires obtaining a closed form solution for the system of equations (2):

$$\begin{cases} X = X(x,y,z) \\ Y = Y(x,y,z) \\ Z = Z(x,y,z) \end{cases} \tag{8}$$

satisfying uniqueness and orthogonality conditions:

$$J = \begin{vmatrix} X_{,x} & Y_{,x} & Z_{,x} \\ X_{,y} & Y_{,y} & Z_{,y} \\ X_{,z} & Y_{,z} & Z_{,z} \end{vmatrix} \neq 0 \tag{9}$$

$$\begin{cases} X_{,x}X_{,y} + Y_{,x}Y_{,y} + Z_{,x}Z_{,y} = 0 \\ X_{,z}X_{,y} + Y_{,z}Y_{,y} + Z_{,z}Z_{,y} = 0 \\ X_{,x}X_{,z} + Y_{,x}Y_{,z} + Z_{,x}Z_{,z} = 0 \end{cases} \tag{10}$$

Then, a family of non-intersecting streamlines can be associated with the x-coordinate lines. We shall first consider a class of velocity fields such that each streamline in the field lies entirely within some plane, referring to these fields as *planar* velocity fields. In planar velocity fields the condition that streamlines should never intersect can be most easily satisfied in the following two cases:

Case I: *Plane* velocity fields—where all the planes are parallel to each other;
Case II: *Radial* velocity fields—where all the planes intersect along the same straight line.

These cases are considered separately below.

2.2. Plane velocity fields

Let us choose the Z-axis of the Cartesian coordinate system in such a way that all the planes containing streamlines are orthogonal to it. In this case the coordinate surface z is a plane given by $z = Z - Z_0$, so that $Z_{,x} = Z_{,y} = 0$ and $Z_{,z} = 1$. The uniqueness condition (9) becomes

$$X_{,x}Y_{,y} - Y_{,x}X_{,y} \neq 0 \tag{11}$$

and it follows that, in order to have a non-trivial solution, orthogonality conditions (10) must be reduced to:

$$\begin{cases} X_{,x}X_{,y} + Y_{,x}Y_{,y} = 0 \\ X_{,z} = Y_{,z} = 0 \end{cases} \tag{12}$$

Let us consider some simple coordinate transformations satisfying both uniqueness (11) and orthogonality conditions (12).

Example 2.2.1 (*Straight streamlines*). Consider coordinate surfaces x, y and z given by expressions

$$\begin{cases} x = (X - X_0)\cos\psi + (Y - Y_0)\sin\psi \\ y = (Y - Y_0)\cos\psi - (X - X_0)\sin\psi \\ z = Z - Z_0 \end{cases} \tag{13}$$

Intersection of a family of coordinate surfaces y with a plane z produces a family of straight parallel streamlines, inclined to any $Y =$ const. plane by angle ψ. When Eqs. (13) are resolved, they produce:

$$\begin{cases} X = X_0 + x\cos\psi - y\sin\psi \\ Y = Y_0 + x\sin\psi + y\cos\psi \\ Z = Z_0 + z \end{cases} \tag{14}$$

From Eqs. (5) it follows that $\alpha = \beta = \gamma = 1$ and from Eq. (7): $u = f(y,z)$ is some function of coordinates y and z describing a particular velocity field, satisfying the incompressibility condition for any smooth f.

Example 2.2.2 (*Circular streamlines*). Consider coordinate surfaces x, y and z given by expressions

$$\begin{cases} x = \arctan\dfrac{Y - Y_0}{X - X_0} \\ y = \sqrt{(Y - Y_0)^2 + (X - X_0)^2} \\ z = Z - Z_0 \end{cases} \tag{15}$$

Intersection of a family of coordinate surfaces y with the plane z produces a family of circular concentric streamlines, which are centered at the point $\{X_0, Y_0\}$. When Eqs. (15) are resolved, they produce:

$$\begin{cases} X = X_0 + y\cos x \\ Y = Y_0 + y\sin x \\ Z = Z_0 + z \end{cases} \tag{16}$$

From Eqs. (5) it follows that $\alpha = y$ and $\beta = \gamma = 1$ and from Eq. (7) $u = f(y,z)$ satisfies the incompressibility condition for any smooth f.

2.3. Radial velocity fields

Let us choose the Y-axis of the Cartesian coordinate system in such a way that it belongs to all the planes containing streamlines. In this case the coordinate surface z is a plane given by $Z = X \tan z$, so that

$$\begin{cases} Z_{,x} = X_{,x} \tan z \\ Z_{,y} = X_{,y} \tan z \\ Z_{,z} = X_{,z} \tan z + X(1 + \tan^2 z) \end{cases} \tag{17}$$

The uniqueness condition (9) becomes

$$\begin{cases} X_{,x}Y_{,y} - Y_{,x}X_{,y} \neq 0 \\ X \neq 0 \end{cases} \tag{18}$$

and it follows, that in order to have a non-trivial solution, orthogonality conditions (10) must be reduced to:

$$\begin{cases} X_{,x}X_{,y}(1 + \tan^2 z) + Y_{,x}Y_{,y} = 0 \\ X_{,z} = -X \tan z \\ Y_{,z} = 0 \end{cases} \tag{19}$$

Two simple examples satisfying these conditions are considered below.

Example 2.3.1 (*Straight streamlines*). Consider coordinate surfaces x, y and z given by expressions

$$\begin{cases} x = \left(\sqrt{X^2 + Z^2} - R_0\right) \cos\psi + (Y - Y_0) \sin\psi \\ y = (Y - Y_0) \cos\psi - \left(\sqrt{X^2 + Z^2} - R_0\right) \sin\psi \\ z = \arctan(Z/X) \end{cases} \tag{20}$$

Intersection of a family of coordinate surfaces y with a plane $Z = X \tan z$ produces a family of straight parallel streamlines, inclined to any $Y =$ const. plane by angle ψ. When Eqs. (20) are resolved, they produce:

$$\begin{cases} X = (x \cos\psi - y \sin\psi + R_0) \cos z \\ Y = Y_0 + x \sin\psi + y \cos\psi \\ Z = (x \cos\psi - y \sin\psi + R_0) \sin z \end{cases} \tag{21}$$

From Eqs. (5) it follows that $\alpha = \beta = 1$ and $\gamma = x \cos\psi - y \sin\psi + R_0$ and from Eq. (7) $u = f(y,z)/(x \cos\psi - y \sin\psi + R_0)$ satisfies the incompressibility condition for any smooth f.

Example 2.3.2 (*Circular streamlines*). Consider coordinate surfaces x, y and z given by expressions

$$\begin{cases} x = \arctan \dfrac{Y - Y_0}{\sqrt{X^2 + Z^2} - R_0} \\ y = (Y - Y_0) \cos\psi - \left(\sqrt{X^2 + Z^2} - R_0\right) \sin\psi \\ z = \arctan \dfrac{Z}{X} \end{cases} \tag{22}$$

Intersection of a family of coordinate surfaces y with a plane $Z = X \tan z$ produces a family of circular concentric streamlines, which are centered at the points $\{R_0 \cos z, Y_0, R_0 \sin z\}$. When Eqs. (22) are resolved, they produce:

$$\begin{cases} X = (y\cos x + R_0)\cos z \\ Y = Y_0 + y\sin x \\ Z = (y\cos x + R_0)\sin z \end{cases} \tag{23}$$

From Eqs. (5) it follows that $\alpha = y$, $\beta = 1$ and $\gamma = y\cos x + R_0$, so that from Eq. (7) $u = f(y,z)/(y\cos x + R_0)$ satisfies the incompressibility condition for any smooth f.

2.4. Discussion

The general framework presented above allows for derivation of the 3-dimensional KAVFs from any unique orthogonal transformation of Cartesian coordinates $\{X, Y, Z\}$. Straight and circular streamline shapes have been considered, but other shapes are possible, for example involute, hyperbolic, etc. (Puzrin and Randolph, 2003). It is also possible to derive new plane but non-plane-strain KAVFs and radial but non-axisymmetric KAVFs. However, because the curvilinear coordinates used in this method are orthogonal, derivation of arbitrary planar 3-dimensional KAVFs is not possible. For example, plane fields cannot be derived for footing shapes other than a strip, while radial fields cannot be derived for footing shapes other than circular, because for a planar field this would violate orthogonality between the z-coordinate axis and xoy plane.

The purpose of this paper is to extend the above approach to allow for a greater flexibility in generation of the new planar KAVFs, in particular plane fields for a circular footing or radial fields for arbitrarily shaped footings. This extension can be easily accommodated by allowing for parameters X_0, Y_0, Z_0, R_0 and ψ in coordinate transformations (14), (16), (21) and (23) to be some functions of z. Unfortunately, such modifications result in these transformations becoming non-orthogonal, and the strain-rate tensor cannot be expressed in the simple form (4) any more. Of course, there is a formal way to treat non-orthogonal curvilinear transformations of coordinates and to derive corresponding components of the strain-rate tensor (Sedov, 1973). Unfortunately, this general approach results in rather monstrous relationships for strain-rate tensor components, which are unlikely to result in closed form expressions for the local dissipation of plastic work. Bearing in mind that the objective of this study is to introduce more realistic shapes of KAVFs, while maintaining simplicity and clear engineering meaning of the upper bound solutions, it is essential to minimise complexity.

3. Simplified technique for non-orthogonal planar fields

This section offers a simplified technique for derivation of the plastic strain-rate tensor and of the local dissipation of plastic work for some types of planar velocity fields, which cannot be obtained using orthogonal curvilinear coordinates. The technique will be applied to fields with straight and circular streamlines, although it is developed in a general form to include other shapes as well.

3.1. Non-orthogonal curvilinear coordinates

Consider a curvilinear orthogonal coordinate system (2) with a functional dependence on parameter t:

$$\begin{cases} x = x(X, Y, Z, t) \\ y = y(X, Y, Z, t) \\ z = z(X, Y, Z, t) \end{cases} \tag{24}$$

where X, Y and Z are Cartesian coordinates:

$$\begin{cases} X = X(x, y, z, t) \\ Y = Y(x, y, z, t) \\ Z = Z(x, y, z, t) \end{cases} \tag{25}$$

When parameter t is independent of coordinates, the coordinate system (24) is orthogonal and the approach described in the previous section applies. Modification of this approach will be achieved by identifying parameter t with curvilinear coordinate z, resulting in the coordinate system (24) becoming non-orthogonal. However, for sake of formality, it is useful to keep them as two separate variables till later stages. The original velocity field, when presented in curvilinear coordinates (x, y, z), is given by the vector:

$$\mathbf{v} = ue_x + ve_y + we_z \tag{26}$$

where $u = u(x, y, z, t)$, $v = v(x, y, z, t)$, $w = w(x, y, z, t)$ are the corresponding components of the velocity field; $e_x(x, y, z, t)$, $e_y(x, y, z, t)$ and $e_z(x, y, z, t)$ are unit coordinate vectors in coordinate directions x, y and z, respectively (Boresi and Chong, 2000):

$$e_x = \frac{r_x}{\alpha} \quad e_y = \frac{r_y}{\beta} \quad e_z = \frac{r_z}{\gamma} \tag{27}$$

where $r(x, y, z, t) = \{X(x, y, z, t), Y(x, y, z, t), Z(x, y, z, t)\}^{\mathrm{T}}$ is a radius-vector defining the position of the point in Cartesian coordinates, so that

$$r_x(x, y, z, t) = \begin{Bmatrix} X_{,x} \\ Y_{,x} \\ Z_{,x} \end{Bmatrix} \quad r_y(x, y, z, t) = \begin{Bmatrix} X_{,y} \\ Y_{,y} \\ Z_{,y} \end{Bmatrix} \quad r_z(x, y, z, t) = \begin{Bmatrix} X_{,z} \\ Y_{,z} \\ Z_{,z} \end{Bmatrix} \tag{28}$$

$$\begin{aligned} \alpha(x, y, z, t) &= \sqrt{r_x \cdot r_x} = \sqrt{(X_{,x})^2 + (Y_{,x})^2 + (Z_{,x})^2} \\ \beta(x, y, z, t) &= \sqrt{r_y \cdot r_y} = \sqrt{(X_{,y})^2 + (Y_{,y})^2 + (Z_{,y})^2} \\ \gamma(x, y, z, t) &= \sqrt{r_z \cdot r_z} = \sqrt{(X_{,z})^2 + (Y_{,z})^2 + (Z_{,z})^2} \end{aligned} \tag{29}$$

Like in the previous section, we consider curvilinear coordinates (x, y, z) such that the x-axis (given by intersection between coordinate surfaces y and z) is directed down the streamline of the velocity field, i.e. $v = w = 0$. If parameter t was independent of (x, y, z), this coordinate system would remain orthogonal and the small strain rate tensor would be given by (4).

When parameter t does change with curvilinear coordinates (x, y, z), in particular $t = z$, this coordinate system will not be orthogonal, so that the strain components derived from the velocity field $\mathbf{v} = ue_x$ will be affected by these changes. Thus

$$\frac{\mathrm{d}\mathbf{v}}{\mathrm{d}t} = \left(\frac{\mathrm{d}u}{\mathrm{d}t} e_x + u \frac{\mathrm{d}e_x}{\mathrm{d}t} \right)_{t=z} \tag{30}$$

where

$$\frac{\mathrm{d}u}{\mathrm{d}t} = u_{,x}x_{,t} + u_{,y}y_{,t} + u_{,z}z_{,t} + u_{,t} \tag{31}$$

$$\frac{\mathrm{d}e_x}{\mathrm{d}t} = e_{xx}x_{,t} + e_{xy}y_{,t} + e_{xz}z_{,t} + e_{xt} \tag{32}$$

where $x_{,t}$ and $y_{,t}$ are obtained by differentiating expressions (24) with respect to t and subsequent substitution of expressions (25) into them, while $z_{,t}|_{t=z} = 1$.

From Boresi and Chong (2000) and relations (27) it follows that

$$e_{xx} = -\frac{\alpha_{,y}}{\beta}e_y - \frac{\alpha_{,z}}{\gamma}e_z \quad e_{xy} = \frac{\beta_{,x}}{\alpha}e_y \quad e_{xz} = \frac{\gamma_{,x}}{\alpha}e_z \tag{33}$$

Substitution of Eqs. (31)–(33) into (30) yields:

$$\left.\frac{\mathrm{d}\mathbf{v}}{\mathrm{d}t}\right|_{t=z} = (u_{,x}x_{,t} + u_{,y}y_{,t} + u_{,z} + u_{,t} + ue_{xt}e_x)_{t=z}e_x + \left(-\alpha_{,y}\frac{u}{\beta}x_{,t} + \beta_{,x}\frac{u}{\alpha}y_{,t} + ue_{xt}e_y\right)_{t=z}e_y + \left(-\alpha_{,z}\frac{u}{\gamma}x_{,t} + \gamma_{,x}\frac{u}{\alpha} + ue_{xt}e_z\right)_{t=z}e_z \tag{34}$$

From $e_xe_x = 1$ it follows that $e_{xt}e_x = 0$. Next, using orthogonality conditions (12) for plane fields and conditions (17) and (19) for radial fields it can be easily shown that for any planar field: $e_{xt}e_z = 0$ and $\alpha_{,z} = 0$, so that Eqs. (34) can be further simplified:

$$\frac{1}{\gamma}\left.\frac{\mathrm{d}\mathbf{v}}{\mathrm{d}t}\right|_{t=z} = \frac{1}{\gamma}(u_{,x}x_{,t} + u_{,y}y_{,t} + u_{,z} + u_{,t})_{t=z}e_x + \frac{u}{\gamma}\left(\frac{\beta_{,x}}{\alpha}y_{,t} - \frac{\alpha_{,y}}{\beta}x_{,t} + \frac{\omega}{\alpha\beta}\right)_{t=z}e_y + \frac{\gamma_{,x}}{\gamma}\frac{u}{\alpha}e_z \tag{35}$$

where

$$\omega = X_{,xt}X_y + Y_{,xt}Y_y + Z_{,xt}Z_y \tag{36}$$

The left hand side of Eq. (35) can be expressed as:

$$\frac{1}{\gamma}\left.\frac{\mathrm{d}\mathbf{v}}{\mathrm{d}t}\right|_{t=z} = 2\dot{\varepsilon}_{xz}e_x + 2\dot{\varepsilon}_{yz}e_y + \dot{\varepsilon}_z e_z \tag{37}$$

Expressions (35)–(37) and (4) then yield the following strain rate tensor components for a planar field depending on the parameter $t = z$:

$$\begin{aligned} &\dot{\varepsilon}_x = \frac{u_{,x}}{\alpha} \quad \dot{\varepsilon}_{xy} = \frac{\alpha}{2\beta}\left(\frac{u}{\alpha}\right)_{,y} \\ &\dot{\varepsilon}_y = \frac{\beta_{,x}}{\beta}\frac{u}{\alpha} \quad \dot{\varepsilon}_{yz} = \frac{u}{2\gamma}\left(\frac{\beta_{,x}}{\alpha}y_{,t} - \frac{\alpha_{,y}}{\beta}x_{,t} + \frac{\omega}{\alpha\beta}\right)_{t=z} \\ &\dot{\varepsilon}_z = \frac{\gamma_{,x}}{\gamma}\frac{u}{\alpha} \quad \dot{\varepsilon}_{xz} = \frac{1}{2\gamma}(u_{,x}x_{,t} + u_{,y}y_{,t} + u_{,z} + u_{,t})_{t=z} \end{aligned} \tag{38}$$

Obviously, for cases when a planar velocity field can be expressed using curvilinear coordinates that do not dependent on parameter t, the strain rate tensor (38) degenerates into expression (4).

The incompressibility condition is still given by Eq. (6), yielding the following functional form for the velocity component u:

$$u(x,y,z,t) = \frac{f(y,z)}{\beta(x,y,z,t)\gamma(x,y,z,t)} \tag{39}$$

where $f(y,z)$ is an arbitrary function of y and z. It follows that the incompressibility condition does not place any restrictions on variation of the velocity with y- and z-coordinates, but its variation with the x-coordinate depends on the functional form of β and γ.

The characteristic equation for the strain rate tensor (38), satisfying condition (6), is given by:

$$\dot{\varepsilon}^3 - p\dot{\varepsilon} + q = 0 \tag{40}$$

where

$$p = -\begin{vmatrix} \dot{\varepsilon}_x & \dot{\varepsilon}_{xy} \\ \dot{\varepsilon}_{yx} & \dot{\varepsilon}_y \end{vmatrix} - \begin{vmatrix} \dot{\varepsilon}_y & \dot{\varepsilon}_{yz} \\ \dot{\varepsilon}_{zy} & \dot{\varepsilon}_z \end{vmatrix} - \begin{vmatrix} \dot{\varepsilon}_x & \dot{\varepsilon}_{xz} \\ \dot{\varepsilon}_{zx} & \dot{\varepsilon}_z \end{vmatrix} \tag{41}$$

$$q = \begin{vmatrix} \dot{\varepsilon}_x & \dot{\varepsilon}_{xy} & \dot{\varepsilon}_{xz} \\ \dot{\varepsilon}_{yx} & \dot{\varepsilon}_y & \dot{\varepsilon}_{yz} \\ \dot{\varepsilon}_{zx} & \dot{\varepsilon}_{zy} & \dot{\varepsilon}_z \end{vmatrix} \tag{42}$$

When $p > 0$, the absolutely largest value of the principal strain rate is obtained in closed form after solving the cubic equation (40):

$$|\dot{\varepsilon}|_{\max} = \sqrt{\frac{p}{3}} \cos\left(\frac{1}{3}\arccos\frac{3\sqrt{3}|q|}{2\sqrt{p^3}}\right) \tag{43}$$

By substituting expression (43) into Eq. (1) and expressing an infinitesimal volume in curvilinear orthogonal coordinates

$$\mathrm{d}V = \alpha\beta\gamma\,\mathrm{d}x\,\mathrm{d}y\,\mathrm{d}z \tag{44}$$

we can calculate the volume integral in Eq. (1) using simple numerical or analytical integration.

The surface integral in Eq. (1) is taken over the discontinuity surfaces. In many cases these discontinuity surfaces coincide with the coordinate surfaces x, y or z. Then the infinitesimal area of discontinuity surface is given by one of the following three expressions:

$$\mathrm{d}S_x = \beta\gamma\,\mathrm{d}y\,\mathrm{d}z \quad \mathrm{d}S_y = \alpha\gamma\,\mathrm{d}x\,\mathrm{d}z \quad \mathrm{d}S_z = \alpha\beta\,\mathrm{d}x\,\mathrm{d}y \tag{45}$$

where $\mathrm{d}S_x, \mathrm{d}S_y$ and $\mathrm{d}S_z$ are the infinitesimal areas of the coordinate surfaces x, y and z, respectively. The velocity jump Δv across the discontinuity is calculated as a vector difference between the tangential components of the two velocity vectors at both sides of discontinuity. When the discontinuity coincides with the coordinate surface x, one of these two vectors is perpendicular to the discontinuity and its tangential component is zero. In cases when the discontinuity coincides with the coordinate surface y or z, one of these two vectors lies entirely within the discontinuity; its tangential component is parallel to the x-coordinate line and has a length u, defined by expression (39). This simplifies expression for $|\Delta v|$ in the surface integral in Eq. (1), allowing for simple numerical or analytical integration.

As is seen from the above derivations, utilisation of a curvilinear orthogonal coordinate system simplifies integration of the rate of dissipation of plastic work. Subsequently, the upper bound surface traction can be easily calculated for the chosen planar KAVF.

3.2. Plane velocity fields

Let us consider examples of application of the above approach to the plane velocity fields described in Section 2.2.

Example 3.2.1 (*Straight streamlines*). Consider a velocity field defined by coordinate transformations (13) and (14), where parameters X_0, Y_0 and ψ are some functions of z. From Eqs. (5), (36), (39) it follows that $\alpha = \beta = \gamma = 1$, $\omega = \psi'(t)$ and $u = f(y,z)$. From Eqs. (13) and (14) we obtain:

$$\begin{cases} x_{,t} = y\psi'(t) - X_0'(t)\cos\psi(t) - Y_0'(t)\sin\psi(t) \\ y_{,t} = -x\psi'(t) + X_0'(t)\sin\psi(t) - Y_0'(t)\cos\psi(t) \end{cases} \tag{46}$$

so that the strain rate tensor (38) becomes:

$$\begin{array}{ll} \dot{\varepsilon}_{x=0} & \dot{\varepsilon}_{xy} = f_{,y}/2 \\ \dot{\varepsilon}_{y=0} & \dot{\varepsilon}_{yz} = f\psi'(z)/2 \\ \dot{\varepsilon}_{z=0} & \dot{\varepsilon}_{xz} = f_{,z}/2 + f_{,y}(-x\psi'(z) + X_0'(z)\sin\psi(z) - Y_0'(z)\cos\psi(z))/2 \end{array} \tag{47}$$

From Eqs. (41) and (42) we obtain:

$$\begin{cases} p = \dot{\varepsilon}_{xy}^2 + \dot{\varepsilon}_{yz}^2 + \dot{\varepsilon}_{xz}^2 > 0 \\ q = 2\dot{\varepsilon}_{xy}\dot{\varepsilon}_{yz}\dot{\varepsilon}_{xz} \end{cases} \tag{48}$$

and the absolutely largest value of the principal strain rate is obtained from Eq. (43). In the particular case of $\psi = \text{const.}$:

$$|\dot{\varepsilon}|_{\max} = \sqrt{\dot{\varepsilon}_{xy}^2 + \dot{\varepsilon}_{xz}^2} \tag{49}$$

Example 3.2.2 (*Circular streamlines*). Consider a velocity field defined by coordinate transformations (15) and (16), where parameters X_0 and Y_0 are some functions of z. From Eqs. (5), (36), (39) it follows that $\alpha = y$, $\beta = \gamma = 1$, $\omega = 0$ and $u = f(y,z)$. From Eqs. (15) and (16), we obtain:

$$\begin{cases} x_{,t} = \dfrac{X_0'(t)\sin x - Y_0'(t)\cos x}{y} \\ y_{,t} = -X_0'(t)\cos x - Y_0'(t)\sin x \end{cases} \tag{50}$$

so that the strain rate tensor (38) becomes:

$$\begin{array}{ll} \dot{\varepsilon}_x = 0 & \dot{\varepsilon}_{xy} = f/(2y) - f_{,y}/2 \\ \dot{\varepsilon}_y = 0 & \dot{\varepsilon}_{yz} = f(Y_0'(z)\cos x - X_0'(z)\sin x)/(2y) \\ \dot{\varepsilon}_z = 0 & \dot{\varepsilon}_{xz} = f_{,z}/2 - f_{,y}(X_0'(z)\cos x + Y_0'(z)\sin x)/2 \end{array} \tag{51}$$

From Eqs. (41) and (42) we obtain again Eq. (48) and the absolutely largest value of the principal strain rate is obtained from Eq. (43). In the particular case of $f = \text{const.}$:

$$|\dot{\varepsilon}|_{\max} = \sqrt{\dot{\varepsilon}_{xy}^2 + \dot{\varepsilon}_{yz}^2} \tag{52}$$

3.3. Radial velocity fields

Finally, let us consider examples of application of the above approach to the radial velocity fields described in Section 2.3.

Example 3.3.1 (*Straight streamlines*). Consider a velocity field defined by coordinate transformations (20) and (21), where parameters R_0, Y_0 and ψ are some functions of z. From Eqs. (5), (36), (39) it follows that $\alpha = \beta = 1$, $\gamma = x\cos\psi(t) - y\sin\psi(t) + R_0(t)$, $\omega = \psi'(t)$ and $u = f(y,z)/(x\cos\psi(t) - y\sin\psi(t) + R_0(t))$. From Eqs. (20) and (21) we obtain:

$$\begin{cases} x_{,t} = y\psi'(t) - R_0'(t)\cos\psi(t) - Y_0'(t)\sin\psi(t) \\ y_{,t} = -x\psi'(t) + R_0'(t)\sin\psi(t) - Y_0'(t)\cos\psi(t) \end{cases} \tag{53}$$

so that the strain rate tensor (38) becomes:

$$\begin{aligned}
&\dot{\varepsilon}_x = -\frac{f\cos\psi(z)}{\gamma^2} \quad \dot{\varepsilon}_{xy} = \frac{f\sin\psi(z) + \gamma f_{,y}}{2\gamma^2} \\
&\dot{\varepsilon}_y = 0 \quad \dot{\varepsilon}_{yz} = f\psi'(z)/(2\gamma^2) \\
&\dot{\varepsilon}_z = \frac{f\cos\psi(z)}{\gamma^2} \quad \dot{\varepsilon}_{xz} = \frac{f_{,z} + f_{,y}(-x\psi'(z) + R_0'(z)\sin\psi(z) - Y_0'(z)\cos\psi(z))}{2\gamma^2}
\end{aligned} \tag{54}$$

From Eqs. (41) and (42) we obtain:

$$\begin{cases} p = \dot{\varepsilon}_{xy}^2 + \dot{\varepsilon}_{yz}^2 + \dot{\varepsilon}_{xz}^2 + \dot{\varepsilon}_z^2 > 0 \\ q = 2\dot{\varepsilon}_{xy}\dot{\varepsilon}_{yz}\dot{\varepsilon}_{xz} + \dot{\varepsilon}_z(\dot{\varepsilon}_{yz}^2 - \dot{\varepsilon}_{xy}^2) \end{cases} \tag{55}$$

and the absolutely largest value of the principal strain rate is obtained from Eq. (43).

Example 3.3.2 (*Circular streamlines*). Consider a velocity field defined by coordinate transformations (22) and (23), where parameters X_0 and Y_0 are some functions of z. From Eqs. (5), (36), (39) it follows that $\alpha = y$, $\beta = 1$, $\gamma = y\cos x + R_0(t)$, $\omega = 0$ and $u = f(y,z)/(y\cos x + R_0(t))$. From Eqs. (22) and (23) we obtain:

$$\begin{cases} x_{,t} = \dfrac{R_0'(t)\sin x - Y_0'(t)\cos x}{y} \\ y_{,t} = -R_0'(t)\cos x - Y_0'(t)\sin x \end{cases} \tag{56}$$

so that the strain rate tensor (38) becomes:

$$\begin{aligned}
&\dot{\varepsilon}_x = \frac{f\sin x}{\gamma^2} \quad \dot{\varepsilon}_{xy} = \frac{y\gamma f_{,y} - (y\cos x + \gamma)f}{2y\gamma^2} \\
&\dot{\varepsilon}_y = 0 \quad \dot{\varepsilon}_{yz} = f(Y_0'(z)\cos x - R_0'(z)\sin x)/(2y\gamma^2) \\
&\dot{\varepsilon}_z = -\frac{f\sin x}{\gamma^2} \quad \dot{\varepsilon}_{xz} = \frac{f_{,z} - f_{,y}(R_0'(z)\cos x + Y_0'(z)\sin x)}{2\gamma^2}
\end{aligned} \tag{57}$$

From Eqs. (41) and (42) we obtain again Eq. (55) and the absolutely largest value of the principal strain rate is obtained from Eq. (43).

3.4. Discussion

Derivation of KAVFs using the proposed approach has allowed closed form expressions of the maximum absolute values of principal strain rates to be obtained by means of a standard procedure. This will reduce calculations of the upper bounds to simple numerical integration, while in some cases closed form upper bound solutions could be obtained.

However, the benefits of the proposed approach extend far beyond simplifications in calculations. In the following sections we demonstrate two applications of the approach, namely:

- plane KAVF for a circular footing;
- radial KAVF for an arbitrarily shaped footing.

4. Applications: plane fields for a circular footing

In order to demonstrate application of the proposed approach to derivation of non-plane-strain KAVFs, let us consider the bearing capacity problem of a rigid rough circular footing of radius b on undrained

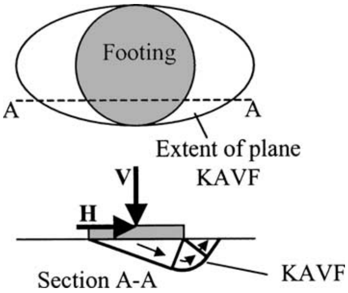

Fig. 1. Schematic of circular footing and associated KAVF.

saturated clay subjected to combined loading by a vertical force **V** and horizontal force **H**. The collapse mechanism is assumed to comprise motion only in the plane of the combined V–H loading, with the extent of the field determined by the width of the footing at any given offset from the center (Fig. 1). The instantaneous velocity of the footing is parallel to the plane of the acting forces **V** and **H** and inclined by angle δ to the surface of the footing, with magnitude of v_0 (Fig. 2). As is seen from Fig. 2a, in a section through a plane parallel to the vertical plane containing the forces **V** and **H**, the field is built of two triangular rigid zones 1 and 3 with straight streamlines, and one fan shear zone 2 with circular streamlines. The Cartesian coordinate system is chosen with the origin at the center of the footing and axis Z perpendicular to the plane of the forces **V** and **H**. The planar mechanism is thus equivalent to the mechanism proposed by Green (1954) for a strip footing.

In rigid zone 1 ($A_tB_tC_t$ in Fig. 2b), a new coordinate system x_1y_1z with the origin at the point B_t is obtained from the transformation (13), with $\psi(t) = \delta = \text{const.}$, $X_0(t) = \sqrt{b^2 - t^2}$ and $Y_0 = Z_0 = 0$. (Note that, as given in Eqs. (14) and (16), the offset coordinate of the field under consideration is $Z = t$, as t is identified with z. The origin of the z-axis always stays in the XOY plane, therefore, $Z_0 = 0$.) A similar transformation, but with $\psi(t) = -\pi/4 = \text{const.}$, yields coordinate system x_3y_3z in rigid zone 3 ($D_tB_tE_t$ in Fig. 2d). Finally, in the fan shear zone 2 ($D_tB_tC_t$ in Fig. 2c), the coordinate system x_2y_2z with the origin at the point B_t is obtained from the transformation (15) with $X_0(t) = \sqrt{b^2 - t^2}$ and $Y_0 = Z_0 = 0$. The velocity

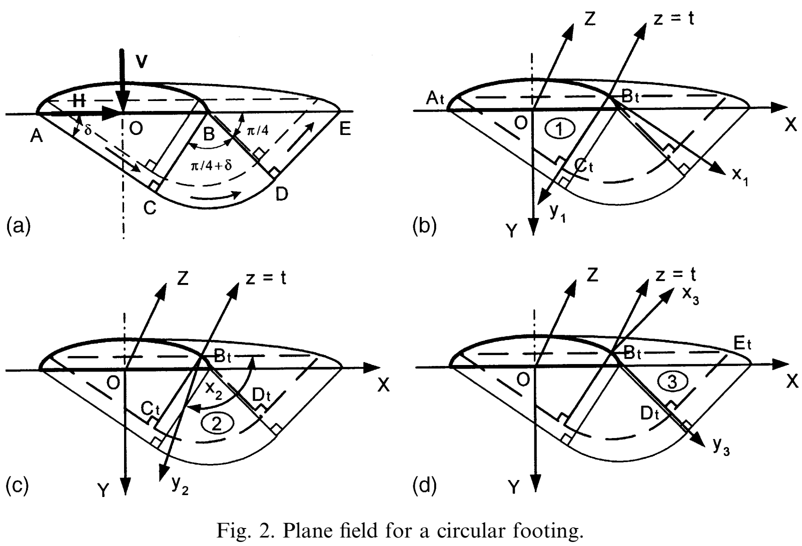

Fig. 2. Plane field for a circular footing.

Table 1
Internal plastic work for circular footing under inclined force loading

		Internal plastic work
Region 1	Volume	$D_1 = 2c_u \int_0^b \int_0^{2\sin\delta\sqrt{b^2-z^2}} \int_{-y_1\cot\delta}^0 \lvert\dot{\varepsilon}\rvert_{\max}\,dx_1\,dy_1\,dz = 0$
	Interface	$D_{A_tC_t} = c_u \int_0^b \int_{-2\cos\delta\sqrt{b^2-z^2}}^0 \lvert\Delta v_1\rvert\,dx_1 \sqrt{1+\frac{z^2\sin^2\delta}{b^2-z^2}}dz = \frac{1}{2}(\sin 2\delta + \pi - 2\delta)b^2c_u v_0$
Region 2	Volume	$D_2 = 2c_u \int_0^b \int_0^{2\sin\delta\sqrt{b^2-z^2}} \int_{\pi/4}^{\pi/2+\delta} \lvert\dot{\varepsilon}\rvert_{\max} y_2\,dx_2\,dy_2\,dz = \left(c - \sin\delta + 0.813532 + \int_0^{\delta}\frac{x}{\sin x}dx\right)b^2c_u v_0 \sin\delta$
	Interface	$D_{C_tD_t} = c_u \int_0^b \int_{\pi/4}^{\pi/2+\delta} \lvert\Delta v_2\rvert 2\sin\delta\sqrt{b^2-z^2}\,dx_2 \sqrt{1+\frac{z^2(2\sin\delta+\cos x_2)^2}{b^2-z^2}}dz = b^2c_u v_0\sin\delta\left(\left(\frac{\pi}{2}+2\delta\right)\sin\delta + \cos\delta - 1/\sqrt{2}\right) + b^2c_u v_0 \sin\delta\begin{Bmatrix} \int_{\sin\delta}^c f_1(x)\,dx & \text{if } c\leqslant 1 \\ \int_{\sin\delta}^1 f_1(x)\,dx + \int_1^c f_2(x)\,dx & \text{if } c>1 \end{Bmatrix}$
Region 3	Volume	$D_3 = 2c_u \int_0^b \int_0^{2\sin\delta\sqrt{b^2-z^2}} \int_0^{y_3} \lvert\dot{\varepsilon}\rvert_{\max}\,dx_3\,dy_3\,dz = 0$
	Interface	$D_{D_tE_t} = c_u \int_0^b \int_0^{2\sin\delta\sqrt{b^2-z^2}} \lvert\Delta v_3\rvert\,dx_3 \sqrt{1+\frac{z^2(2\sin\delta+1/\sqrt{2})^2}{b^2-z^2}}dz = b^2c_u v_0\sin\delta\begin{Bmatrix} c+f_3(c) & \text{if } c<1 \\ c+f_4(c) & \text{if } c>1 \\ 2 & \text{if } c=1 \end{Bmatrix}$

Where
$c = 2\sin\delta + \frac{1}{\sqrt{2}}$; $f_1(x) = \frac{f_3(x)}{\sqrt{1-(2\sin\delta - x)^2}}$; $f_2(x) = \frac{f_4(x)}{\sqrt{1-(2\sin\delta - x)^2}}$; $f_3(x) = \frac{\arcsin\sqrt{1-x^2}}{\sqrt{1-x^2}}$; $f_4(x) = \frac{\ln(x+\sqrt{x^2-1})}{\sqrt{x^2-1}}$.

fields in the three zones are all parallel to the x_i axes, with velocity magnitudes given by $u_i = f_i(y_i, z) = v_0$, where i is the zone number. As expected, using expressions (47) and (49), the maximum principal strain rates are $\lvert\dot{\varepsilon}\rvert_{\max} = 0$ in rigid zones 1 and 3. From expressions (51) and (52) we obtain $\lvert\dot{\varepsilon}\rvert_{\max} = v_0\sqrt{b^2 - z^2\cos^2 x_2}\Big/\left(2y_2\sqrt{b^2-z^2}\right)$ in shear zone 2. On the interfaces A_tC_t, C_tD_t and D_tE_t, there is a tangential velocity jump $\Delta v_i = v_0$. The expressions for the internal plastic work in each zone and the corresponding interfaces are summarized in Table 1. The total plastic work D in the field is calculated by summing the plastic work in each zone (Table 1). Consequently, Eq. (1) can be written for this case as

$$\mathbf{V}v_0\sin\delta + \mathbf{H}v_0\cos\delta = 2D(\delta) \tag{58}$$

In (**V**, **H**) space, expression (58) represents a straight line depending on parameter δ. By varying this parameter we obtain a family of straight lines whose envelope represents an interaction diagram for the forces

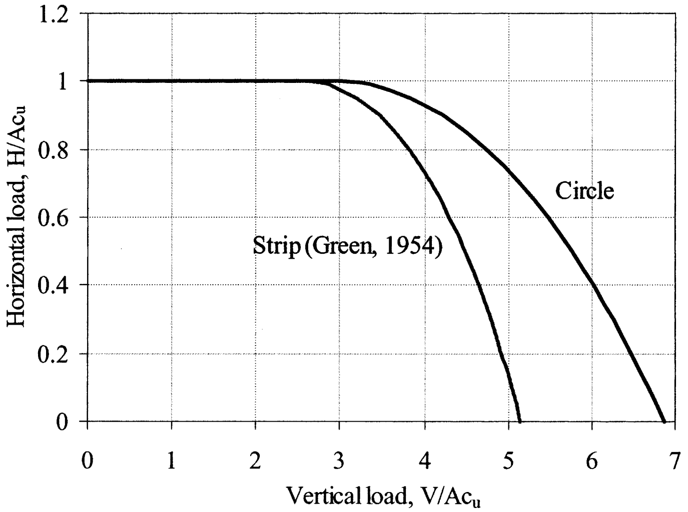

Fig. 3. Upper bound envelopes for strip and circular footings under *V–H* loading.

V and **H**. The resulting envelope is shown in Fig. 3, compared with the plane strain solution of Green (1954) for a strip footing, with V and H normalised by Ac_u, where A is the area of the foundation.

The plane mechanism gives a bearing capacity factor of 6.8 under purely vertical load, which is 13% greater than the exact bearing capacity of 6.05 (Eason and Shield, 1960). The discrepancy can be reduced to 2% through the use of a purely axisymmetric mechanism, but such a mechanism is not useful for combined vertical and horizontal loading. As will be shown in a forthcoming paper, the mechanism proposed here gives the closest known upper bound for values of $\mathbf{H}/\mathbf{V}$ in excess of 0.06, and rapidly merges with the failure envelope obtained from finite element computations as the $\mathbf{H}/\mathbf{V}$ ratio increases further.

5. Applications: radial fields for arbitrarily shaped footings

Levin (1955) proposed an ingenious method for construction of a certain type of non-symmetrical radial KAVFs. However, he was not able to present any results other than those for the axisymmetric case because of the considerable computational complexity of the general case. This complexity resulted mainly from the fact that the velocity fields were formulated in general cylindrical coordinates. The approach proposed in this paper allows for this complexity to be overcome even for more general fields than that proposed by Levin (1955). It allows for the maximum principal strain rate to be obtained in closed form at any point of the field, reducing calculations to simple numerical integration.

To illustrate this approach, let us consider the bearing capacity problem of a smooth footing of arbitrary shape on undrained saturated clay subjected to a loading by a vertical force **V** (Fig. 4). For clarity of presentation, the footing in Fig. 4a has a square shape, but the problem is solved for the case of an arbitrary shape of the footing, which can be described in polar coordinates by some function $d(z)$. The instantaneous velocity of the footing is vertical and its magnitude is equal to v_0. As is seen from Fig. 4b, in a section through a vertical plane containing the center of the footing, the field is built of two triangular shear zones 1 and 3 with straight streamlines, and one fan shear zone 2 with circular streamlines. The Cartesian coordinate system is chosen with the origin at the center of the footing and axis Z in the horizontal plane of the footing. Note that right angles within the KAVF are marked in the conventional way.

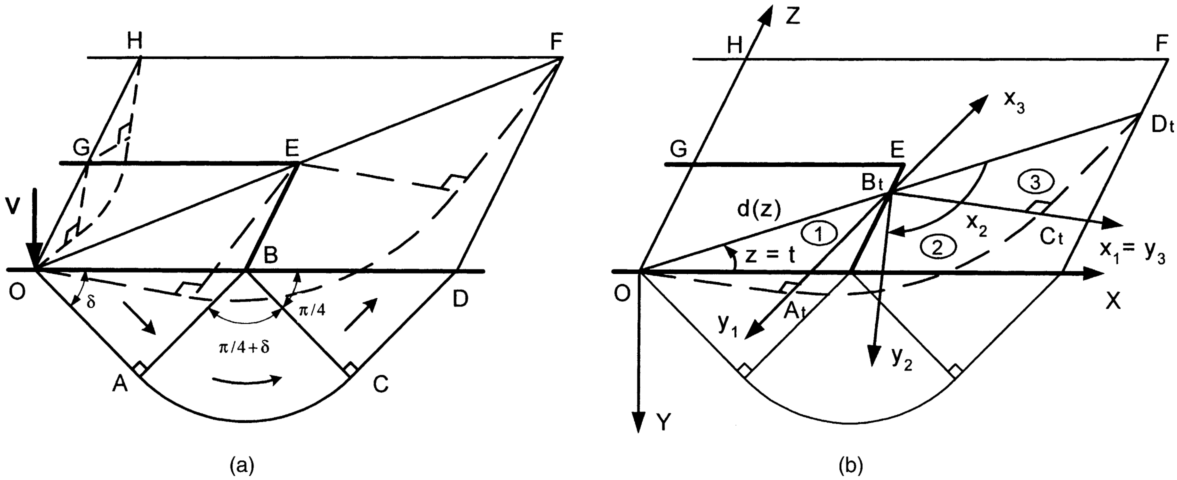

Fig. 4. Radial field for a square footing.

In shear zone 1 (OA_tB_t in Fig. 4b), a new coordinate system x_1y_1z with the origin at the point B_t is obtained from the transformation (20), with $\psi(t) = \delta = \text{const.}$, $R_0(t) = d(t)$ and $Y_0 = 0$. A similar transformation, but with $\psi(t) = -\pi/4 = \text{const.}$, yields coordinate system x_3y_3z in shear zone 3 ($B_tC_tD_t$ in Fig. 4b). Finally, in the fan shear zone 2 ($A_tB_tC_t$ in Fig. 4b), the coordinate system x_2y_2z with the origin at the point B_t is obtained from the transformation (22) with $R_0(t) = d(t)$ and $Y_0 = 0$.

The velocity fields in the three zones are all parallel to the x_i axes, where i is the zone number. Velocity magnitudes in each zone can be defined using expression (7) and velocity continuity conditions on the boundaries between the zones. In shear zone 1, $u_1(x_1, y_1, z) = f_1(y_1, z)/\gamma_1(x_1, y_1, z)$, where $\gamma_1(x_1, y_1, z) = x_1 \cos\delta - y_1 \sin\delta + d(z)$, and at the contact of the footing, where $x_1 = -y_1 \cot\delta$, the velocity boundary condition can be expressed as

$$u_1(-y_1, y_1, z) = f_1(y_1, z)/(-y_1/\sin\delta + d(z)) = v_0/\sin\delta$$

so that

$$f_1(y_1, z) = v_0(d(z) - y_1/\sin\delta)/\sin\delta \tag{59}$$

$$u_1(x_1, y_1, z) = \frac{v_0(d(z) - y_1/\sin\delta)/\sin\delta}{x_1\cos\delta - y_1\sin\delta + d(z)} \tag{60}$$

From Eq. (60) it follows that along the surface OA_t, where $y_1 = d(z)\sin\delta$, the velocity is given by $u_1 = 0$, i.e. there is no velocity discontinuity across this surface.

In shear zone 2, we can describe the velocity as $u_2(x_2, y_2, z) = f_2(y_2, z)/\gamma_2(x_2, y_2, z)$, where $\gamma_2(x_2, y_2, z) = y_2 \cos x_2 + d(z)$ and at the boundary between the zones 1 and 2, where $x_1 = 0$, $x_2 = \pi/2 + \delta$ and $y_1 = y_2$, the velocity continuity condition can be expressed as

$$u_1(0, y_2, z) = f_1(y_2, z)/(-y_2\sin\delta + d(z)) = u_2(\pi/2 + \delta, y_2, z) = f_2(y_2, z)/(-y_2\sin\delta + d(z))$$

so that

$$f_2(y_2, z) = v_0(d(z) - y_2/\sin\delta)/\sin\delta \tag{61}$$

$$u_2(x_2, y_2, z) = \frac{v_0((d(z) - y_2/\sin\delta)/\sin\delta}{y_2\cos x_2 + d(z)} \tag{62}$$

From Eq. (62) it follows that along the surface A_tC_t, where $y_2 = d(z)\sin\delta$, the velocity is given by $u_2 = 0$, i.e. there is no velocity discontinuity across this surface.

Finally, in shear zone 3, the velocity is given by $u_3(x_3, y_3, z) = f_3(y_3, z)/\gamma_3(x_3, y_3, z)$, where $\gamma_3(x_3, y_3, z) = x_3/\sqrt{2} + y_3/\sqrt{2} + d(z)$ and at the boundary between the zones 2 and 3, where $x_3 = 0$, $x_2 = \pi/4$ and $y_3 = y_2$, the velocity continuity condition can be expressed as

$$u_3(0, y_3, z) = \sqrt{2}f_3(y_3, z)/\left(y_3 + \sqrt{2}d(z)\right) = u_2(\pi/4, y_3, z) = \sqrt{2}f_2(y_3, z)/\left(y_3 + \sqrt{2}d(z)\right)$$

so that

$$f_3(y_3, z) = v_0(d(z) - y_3/\sin\delta)/\sin\delta \tag{63}$$

$$u_3(x_3, y_3, z) = \frac{\sqrt{2}v_0(d(z) - y_3/\sin\delta)/\sin\delta}{\sqrt{2}d(z) + x_3 + y_3} \tag{64}$$

From Eq. (64) it follows that along the surface C_tA_t, where $y_2 = d(z)\sin\delta$, the velocity is given by $u_3 = 0$, i.e. there is no velocity discontinuity across this surface as well.

Substitution of Eqs. (59) and (63) into Eqs. (54) yields expressions for strain rate tensor components in shear zones 1 and 3, respectively, while substitution of Eq. (61) into Eqs. (57) yields expressions for strain rate tensor components in shear zones 2. These expressions are summarized in Table 2. By substituting these expressions into Eqs. (55) and (43) we obtain the maximum principal strain rates, $|\dot{\varepsilon}|_{\max i}$, for each of the three shear zones (where i is the number of the shear zone). These expressions are obtained in closed form and are not presented here for the sake of brevity. The total plastic work D in the field is calculated by summing the plastic work in each zone, so that Eq. (1) in our case can be written as

$$\begin{aligned}\mathbf{V}v_0 = {} & 2c_u \int_0^{2\pi}\int_0^{d(z)\sin\delta}\int_{-y_1\cot\delta}^{0} |\dot{\varepsilon}|_{\max 1}(d(z) + x\cos\delta - y\sin\delta)\,dx_1\,dy_1\,dz \\ & + 2c_u \int_0^{2\pi}\int_0^{d(z)\sin\delta}\int_{\pi/4}^{\pi/2+\delta} |\dot{\varepsilon}|_{\max 2}y_2(d(z) + y_2\cos x_2)\,dx_2\,dy_2\,dz \\ & + 2c_u \int_0^{2\pi}\int_0^{d(z)\sin\delta}\int_0^{y_3} |\dot{\varepsilon}|_{\max 3}\left(d(z) + (x_3 + y_3)/\sqrt{2}\right)dx_3\,dy_3\,dz\end{aligned} \tag{65}$$

Table 2
Strain rates for arbitrarily shaped footing under vertical loading

Strain rates	Region 1	Region 2	Region 3
$\dot{\varepsilon}_x$	$-v_0\frac{(d(z)\sin\delta - y)\cos\delta}{\gamma^2\sin^2\delta}$	$v_0\frac{(d(z)\sin\delta - y)\sin x}{\gamma^2\sin^2\delta}$	$-v_0\frac{(d(z)\sin\delta - y)}{\sqrt{2}\gamma^2\sin^2\delta}$
$\dot{\varepsilon}_y$	0	0	0
$\dot{\varepsilon}_z$	$v_0\frac{(d(z)\sin\delta - y)\cos\delta}{\gamma^2\sin^2\delta}$	$-v_0\frac{(d(z)\sin\delta - y)\sin x}{\gamma^2\sin^2\delta}$	$v_0\frac{(d(z)\sin\delta - y)}{\sqrt{2}\gamma^2\sin^2\delta}$
$\dot{\varepsilon}_{xy}$	$-v_0\frac{(d(z)\cos\delta + x)\cos\delta}{2\gamma^2\sin^2\delta}$	$v_0\frac{y^2\cos x - (\gamma + y\cos x)d(z)\sin\delta}{2y\gamma^2\sin^2\delta}$	$-v_0\frac{d(z)(\sqrt{2} + \sin\delta) + x}{2\sqrt{2}\gamma^2\sin^2\delta}$
$\dot{\varepsilon}_{yz}$	0	$-v_0\frac{d'(z)(d(z)\sin\delta - y)\sin x}{2y\gamma^2\sin^2\delta}$	0
$\dot{\varepsilon}_{xz}$	0	$v_0\frac{d'(z)(\sin\delta + \cos x)}{2\gamma^2\sin^2\delta}$	$v_0\frac{d'(z)(\sin\delta + 1/\sqrt{2})}{2\gamma^2\sin^2\delta}$
γ	$d(z) + x\cos\delta - y\sin\delta$	$d(z) + y\cos x$	$d(z) + (x + y)/\sqrt{2}$

For a smooth circular footing with $d(z) = b = \text{const.}$ and $\delta = \pi/4$, Eq. (65) produces $\mathbf{V}/(\pi b^2) = 5.83c_u$, which is identical to the result obtained by Levin (1955). For a smooth square footing of the width and length $2b : d(z) = b/\cos z$, and for the particular case of a Levin type field with $\delta = \pi/4$, Eq. (65) produces $\mathbf{V}/(4b^2) = 6.13c_u$. Levin (1955), though unable to obtain this result, predicted that it was likely to turn out higher than the one for a circular footing, even though the actual bearing capacity for a square footing should be lower than for a circular footing.

6. Concluding remarks

The method of derivation of KAVFs described in this paper extends the recently proposed method based on the use of coordinate transformations. Both the original method and its extension provide significant flexibility for 3-dimensional upper bound solutions in Tresca materials. The main feature of this approach is that it allows the incompressibility condition to be satisfied simply by imposing certain requirements on the analytical form of velocity magnitudes. This allows for new classes of velocity fields to be derived using solely standard procedures. However, while the original method is limited to systems of orthogonal curvilinear coordinates, its extension allows for new classes of fields, which could not be described by orthogonal systems, to be handled within the same framework. These new classes of fields include: new plane but non-plane-strain KAVFs, like a plane field for a circular footing; new radial but non-axisymmetric KAVFs, like a radial field for a square footing.

An additional advantage of the method is that it allows for expression of local dissipation of plastic work in any field to be derived in closed form. When these expressions can be integrated analytically, we obtain analytical solutions for upper bounds of collapse loads, but even numerical integration of these expressions does not constitute a problem of significant complexity and can be easily performed using standard spreadsheets. The proposed method makes an attempt to expand applicability of 3-dimensional upper bound solutions by introducing more realistic shapes of KAVFs, while maintaining the simplicity and clear engineering meaning of this approach.

Acknowledgements

The research was supported by an IREX grant from the Australian Research Council and by the Technion V.P.R. Fund—Sydney Goldstein Research Fund, whose support is gratefully acknowledged. The work contributes to the research program of the Centre for Offshore Foundation Systems at the University of Western Australia, established and supported under the Australian Research Council's Research Centres Program.

References

Boresi, A.P., Chong, K.P., 2000. Elasticity in Engineering Mechanics. John Wiley & Sons, New York.

Drucker, D.C., Greenberg, H.J., Prager, W., 1951. The safety factor of an elastic–plastic body in plane strain. J. Appl. Mech. Trans. ASME 73, 371–378.

Eason, G., Shield, R.T., 1960. The plastic indentation of a semi-infinite solid by a perfectly rough circular punch. J. Appl. Math. Phys. (ZAMP) 11, 33–43.

Green, A.P., 1954. The plastic yielding of metal junctions due to combined shear and pressure. J. Mech. Phys. Solids 2 (3), 197–211.

Levin, A., 1955. Indentation pressure of a smooth circular punch. Quart. Appl. Math. 13, 381–389.

Murff, J.D., Hamilton, J.M., 1993. P-ultimate for undrained analysis of laterally loaded piles. ASCE J. Geotech. Engng. 119 (1), 91–107.

Puzrin, A.M., Randolph, M.F., 2003. Generalised framework for 3D upper bound limit analysis. J. Appl. Mech., ASME.

Sedov, L.I., 1973. In: Mechanics of Continuous Media, vol. 1. Nauka, Moscow (in Russian).

Shield, R.T., Drucker, D.C., 1953. The application of limit analysis to punch indentation problems. J. Appl. Mech. 20, 453–460.